

# Brightening of Dark States in CsPbBr<sub>3</sub> Quantum Dots Caused by Light-Induced Magnetism

Sven-Hendrik Lohmann, Tong Cai, Darien J. Morrow, Ou Chen, and Xuedan Ma\*

Lead halide perovskite quantum dots (QDs) have shown great potential for optoelectronic and quantum photonic applications. Although controversy remains about the electronic fine structures of bulk perovskites due to the strong spin-orbit coupling affecting the conduction bands, compelling evidence indicates that the ground states of perovskite QDs remain dark, limiting their applications in optoelectronic devices. Here, it is demonstrated that photoexcitation can induce large intrinsic magnetic fields in Mn-doped CsPbBr<sub>3</sub> perovskite QDs. Equivalent to applying an external magnetic field, the light-induced field causes giant Zeeman splitting to the bright triplet states and brightens the dark singlet ground state, thus effectively rendering a partially bright ground state in the doped QDs. These findings here may contribute to the understanding of the electronic fine structures in perovskite QDs and demonstrate a potential approach for creating semiconductor nanostructures that can serve as bright light sources.

1. Introduction

Lead halide perovskites are prominent materials showing great potential for applications ranging from optoelectronic devices such as solar cells, light-emitting diodes, and lasers<sup>[1–3]</sup> to spintronic devices.<sup>[4,5]</sup> Inheriting the superior optical and electronic properties of the bulk lead halide perovskites, semiconductor quantum dots (QDs) composed of this group of materials allow composition- and size-tunable narrow-band photoluminescence (PL) and provide additional opportunities for developing stable and efficient optoelectronic devices.<sup>[6]</sup> Moreover, they may serve as nascent single photon sources<sup>[7–9]</sup> for quantum information science. An important aspect related to these applications is the

Dr. S.-H. Lohmann, Dr. D. J. Morrow, Dr. X. Ma
Center for Nanoscale Materials
Argonne National Laboratory
Lemont, IL 60439, USA
E-mail: xuedan.ma@anl.gov
T. Cai, Prof. O. Chen
Department of Chemistry
Brown University
Providence, RI 02912, USA
Dr. X. Ma
Consortium for Advanced Science and Engineering
University of Chicago
Chicago, IL 60637, USA

The ORCID identification number(s) for the author(s) of this article can be found under https://doi.org/10.1002/smll.202101527.

DOI: 10.1002/smll.202101527

electronic fine structure of the perovskite QDs, manifested as bright emission and exceptionally fast exciton decay rates at cryogenic temperatures. [10] For lead halide perovskite QDs with dimensions much larger than their Bohr radius, it remains controversial whether this fast decay rate is caused by a bright triplet ground state due to the Rashba effect [11,12] or suppressed bright-dark state relaxation due to the lack of resonant phonons. [13,14] However, it is widely accepted that the ground states in quantum confined perovskite QDs remain dark singlet, [12,15] akin to other semiconductor nanocrystals.

A constant quest in utilizing light emitting semiconductors such as perovskite QDs for highly efficient optoelectronic devices is to obtain effective conversion between charge carriers and photons while

suppressing any nonradiative recombination processes.[16-18] One of the biggest contributors to this challenge is their optically forbidden ground state,[11,19,20] the long lifetime of which leads to photon losses through parasitic carrier-phonon interactions.<sup>[21]</sup> Various approaches have been developed to diminish such nonradiative recombination processes associated with the optically dark ground states, and activating the lowest-lying dark states using external magnetic fields is one of the most commonly used methods.[13,19,20] A magnetic field can mix an optically forbidden dark state with its energetically neighboring bright states, leading to a finite oscillator strength in the dark state.[13,19,20] However, compared to these approaches relying on external stimuli, design and creation of semiconductor materials with optically bright ground states could help overcome fundamental limitations imposed by the materials' intrinsic photodynamic processes.[22,23]

Equivalent to applying an external magnetic field, light-induced magnetization can exist in semiconductors doped with magnetic ions $^{[24]}$  and lead to Zeeman splitting of their electronic states. $^{[25]}$  In these magnetically doped semiconductors, the strong sp-d exchange interaction between charge carriers and the local magnetic ions can result in the formation of exciton magnetic polarons (EMP). $^{[26,27]}$  During the formation of EMP, photogenerated excitons induce the spontaneous ferromagnetic alignment of the magnetic ions, resulting in the creation of a local ferromagnetic order even in the absence of an external magnetic field (**Figure 1a**). Since the strength of the sp-d exchange interaction scales with the probability density of the exciton wave function at the magnetic ions' locations, the formation of EMP could be much more profound in

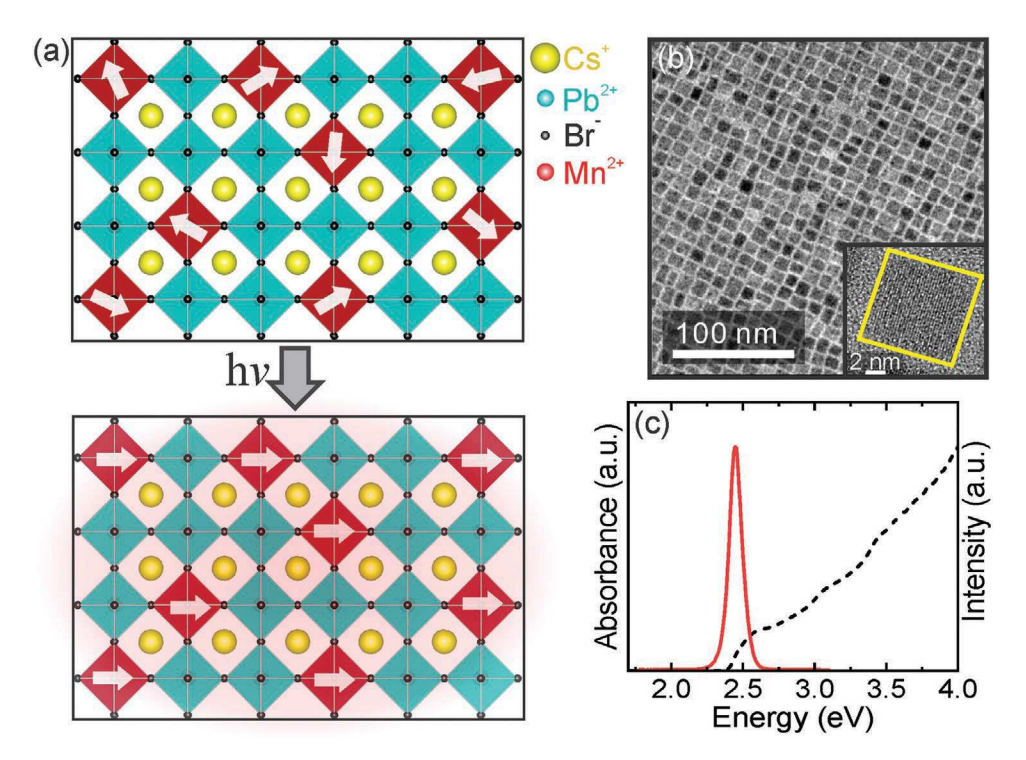


**Figure 1.** Optical and structural properties of the Mn-doped CsPbBr<sub>3</sub> QDs. a) Schematic of the formation of exciton magnetic polarons in the Mn-doped perovskite QDs. b) Transmission electron microscopy (TEM) image of the CsPbBr<sub>3</sub> QDs doped with 6.9% of Mn<sup>2+</sup>-ions. Inset: high-resolution TEM image. c) Absorption (black) and emission (red) spectra of the Mn-doped CsPbBr<sub>3</sub> QDs at room temperature.

quantum confined semiconductor systems due to the localization of the exciton wave functions.<sup>[28]</sup> The effective magnetic field created by EMP has a similar effect to that of an external field and can cause tremendous changes to the electronic fine structures of the host semiconductor nanostructures. The formation of EMP has been reported for a variety of Mn<sup>2+</sup>-ion doped semiconductor systems such as quantum wells,<sup>[29]</sup> self-assembled QDs grown by molecular-beam epitaxy,<sup>[25,30]</sup> and colloidally synthesized QDs.<sup>[24,31]</sup> Most of these studies have focused on doped II–VI or III–V semiconductors, while the investigation of light-induced magnetism in perovskites has remained sparse. Recent developments in the synthesis and doping of perovskite QDs<sup>[32,33]</sup> provide opportunities for such studies.

Here, we demonstrate the formation of a partially bright ground state in Mn-doped CsPbBr3 QDs without the requirement of an external field. We use temperature-dependent optical spectroscopy to investigate the doped QDs and demonstrate the formation of EMP. The substantial effective magnetic field induced by the EMP not only results in giant Zeeman splitting of the bright triplet states in the QDs, but also causes brightening of the dark singlet ground state. These results indicate that the electronic ground state of the Mn-doped CsPbBr<sub>3</sub> QDs used in this study can be switched from dark to a partially bright singlet state without the application of an external magnetic field. This mechanism of creating a bright ground state is applicable to other types of semiconductor nanostructures and provides a versatile approach for obtaining intrinsically bright light emitting materials. The doping-induced control over the bright-dark splitting, and consequently the transition between

them, may promote intriguing optoelectronic applications relying on spin-dependent photophysical processes.<sup>[34–37]</sup>

### 2. Results and Discussion

The CsPbBr3 QDs used in this study were synthesized using a hot-injection method<sup>[38]</sup> and doped with Mn<sup>2+</sup>-ions at concentrations of 1.2%, 1.6%, 4.6%, and 6.9%[39] (see Section S1, Supporting Information for details). Their representative transmission electron microscopy image as well as absorption and emission spectra at room temperature are shown in Figure 1 and Figure S1, Supporting Information, respectively. The average edge length of the QDs is around 10 nm (Figures S2,S3, Supporting Information), which is slightly larger than the exciton Bohr radius of CsPbBr<sub>3</sub> (≈7 nm),<sup>[32]</sup> indicating that the QDs are in the weak quantum confinement regime. This is consistent with their blue-shifted PL spectra compared to their bulk counterparts (Figure 1c).[40] We utilize CsPbBr3 QDs as the hosting material for Mn<sup>2+</sup>-ions in our study because their electronic bandgap is close to the emission energy (d-d transition from  ${}^{4}\mathrm{T}_{1g}$  to  ${}^{6}\mathrm{A}_{1g}$ ) of the Mn<sup>2+</sup>-ions at around 2.1 eV. The relatively small difference between the transition energies of the CsPbBr<sub>3</sub> QDs and the  $\mathrm{Mn^{2+}}\text{-ions}$  (between the  $^{4}\mathrm{T_{1g}}$  and  $^{6}\mathrm{A_{1g}}$  states), together with the characteristic small energy transfer rates in Mn-doped CsPbBr<sub>3</sub> QDs renders energy transfer between these two highly inefficient.[41] This is crucial for the formation of EMP, which requires that the exciton recombination time of the QDs to be longer than the time needed to align the spins of the magnetic ions.[30,42] Prevention of energy transfer from the

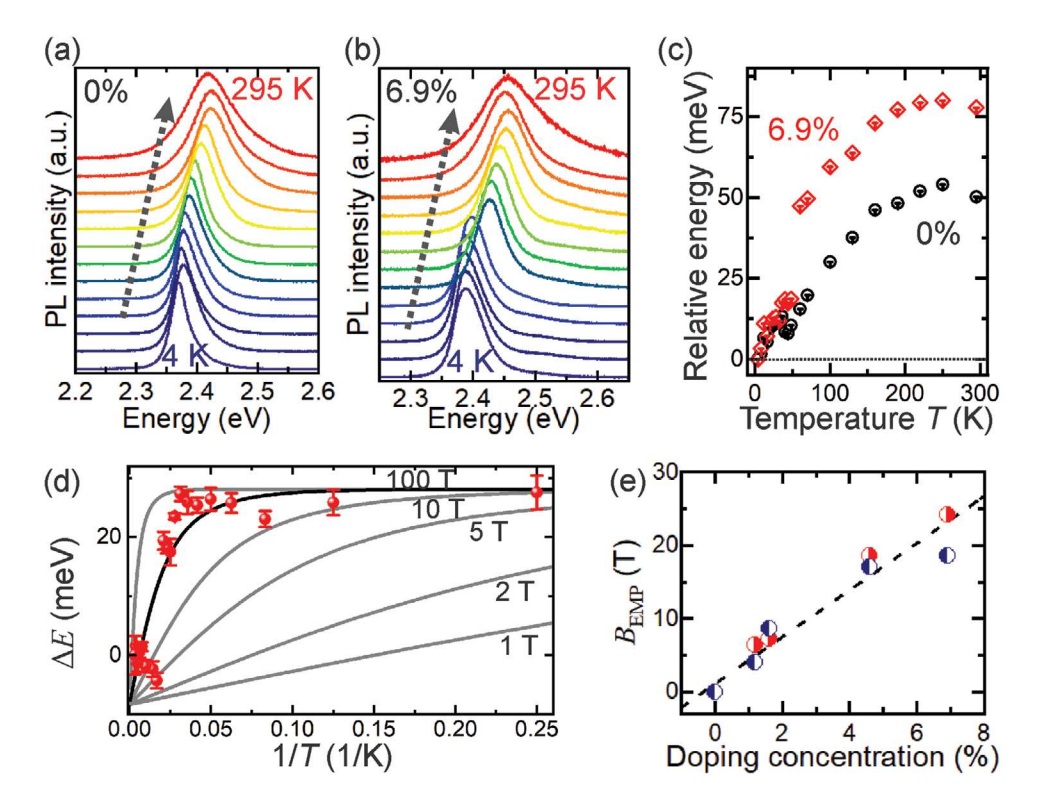


Figure 2. Formation of exciton magnetic polarons in Mn-doped CsPbBr<sub>3</sub> QDs. a,b) Temperature-dependent photoluminescence spectra of CsPbBr<sub>3</sub> QDs doped with 0% (a) and 6.9% (b) Mn<sup>2+</sup>-ions. c) Temperature-dependent emission peak positions of the undoped CsPbBr<sub>3</sub> QDs and those doped with 6.9% Mn<sup>2+</sup>-ions. For clarity, the peak positions are offset by setting the corresponding PL energies at 4 K to zeros. d) Dots: Temperature-dependent energy difference Δ*E* between the undoped QDs and the QDs doped with 6.9% Mn<sup>2+</sup>-ions. The data are offset by setting the Δ*E* value at 4 K to zero. Curves: simulation-obtained Δ*E* values as a function of the temperature by assuming different effective magnetic field  $B_{EMP}$  values in Equation (1). The best fitting result (black curve) is obtained with  $B_{EMP} = 24.2$  T. e) The effective internal magnetic field  $B_{EMP}$  experienced by the QDs with various doping concentrations. The red dots are obtained from the temperature-dependent spectral shifts while the blue dots are from the temperature-dependent lifetime changes. The dashed line is a linear fit to the average  $B_{EMP}$  values.

QDs to the  $Mn^{2+}$ -ions ensures that the formation of the EMP would not be interrupted by exciton recombination.

We investigate the temperature-dependent PL spectra of the CsPbBr<sub>3</sub> QDs doped with various concentrations of Mn<sup>2+</sup>ions using a home-built optical microscope (see Experimental Section). As references, PL spectra of undoped CsPbBr<sub>3</sub> QDs in the temperature range from 4 to 295 K are recorded and shown in Figure 2a. Aside from PL spectral broadening (see Section S2, Supporting Information for details), a continuous blue shift of around 50 meV can also be observed when the temperature increases from 4 to 295 K (Figure 2c, black). This temperature-induced blue shift in the PL peak positions contradicts with the commonly observed Varshni-like red-shift trend observed in other semiconductors. This discrepancy has mainly been attributed to the opposing contributions from different phonon modes in the perovskite QDs. [43] Compared to the undoped CsPbBr<sub>3</sub> QDs, those doped with Mn<sup>2+</sup>-ions also exhibit a blue shift in their PL energies with increasing temperature, although to a larger extent compared to that of the undoped QDs (Figure 2b,c).

Temperature-dependent PL spectral shifts in semiconductors could be related to factors such as lattice expansion and carrier–phonon interactions.<sup>[44,45]</sup> Given the very similar sample conditions including the compositions, sizes, crystalline structures, and surrounding environments of the doped and undoped

QDs, the difference observed in their PL spectra in Figure 2a–c is most likely caused by the doped Mn<sup>2+</sup>-ions. To solely examine the influence of the Mn<sup>2+</sup>-ions on the PL emission and exclude other effects, we use the PL energies of the undoped QDs as reference and calculate the PL energy difference  $\Delta E$  between the undoped and doped QDs. Figure 2d shows the temperature-dependent  $\Delta E$  values for QDs doped with 6.9% of Mn<sup>2+</sup>-ions. The value of  $\Delta E$  remains mostly constant below 30 K but increases drastically with the temperature above 30 K.

Similar temperature-dependent energy shift upon magnetic ion doping has been observed in epitaxial and colloidal II-VI QDs<sup>[24,25,27]</sup> and is attributed to the formation of EMP. Specifically, when the doped QDs are irradiated, photogenerated excitons can induce spontaneous ferromagnetic alignment of the spins in the local Mn<sup>2+</sup>-ions through an exchange field. The resultant aligned magnetic moments act back on the excitons by splitting the excitonic states into Zeeman components. An increase in the temperature may suppress the ordering of the Mn<sup>2+</sup>-ion spins in the QDs due to enhanced random thermal fluctuations. Therefore, the temperature-dependence of the energy difference,  $\Delta E$ , between the undoped and doped QDs could reflect thermally induced changes in the alignment of the Mn<sup>2+</sup>-ion spins.<sup>[24–26]</sup> The PL energy shift caused by the formation of the EMP can be described by a modified Brillouin function:[25,27]

$$\Delta E(T) = CB_{5/2} \left( \frac{5 \,\mu_{\rm B} \,g_{\rm Mn} B}{2k_{\rm p} T} \right) \tag{1}$$

Here, C is a constant related to the doping concentration and exchange parameters of the electrons and holes.  $B_{5/2}$  is the Brillouin function for spin S=5/2. B is the effective internal magnetic field experienced by the doped QDs, which in the absence of an external magnetic field, is mainly contributed by the exchange field of the excitons,  $B_{\rm EMP}$ , due to the sp–d exchange interactions.  $\mu_{\rm B}$  is the Bohr magneton and  $g_{\rm Mn}$  is the g-factor of Mn. In Mn-doped II–VI QDs, exciton exchange fields of up to 17 T have been reported. [31]

Our observation of the temperature-dependent energy shift  $\Delta E$  between the doped and undoped QDs (Figure 2d) is consistent with the formation of EMP in the doped QDs. Using a similar approach as mentioned above to fit the  $\Delta E$  values, we obtain a reasonable agreement between the experimental data and the model when  $B_{\rm EMP} = 24.2~{\rm T}$  (Figure 2d, black curve). The fact that the experimental data can be fit reasonably well up to room temperature indicates that the formed EMP are stable, mainly due to their large binding energies in quantum confined systems.<sup>[46]</sup> We perform similar studies for CsPbBr<sub>3</sub> QDs doped with various concentrations of Mn<sup>2+</sup>-ions and the obtained  $B_{\text{EMP}}$  values are plotted in Figure 2e (red dots). An increase in the doping concentration leads to enhanced sp-d interactions<sup>[47]</sup> and hence larger exciton exchange fields and  $B_{\rm EMP}$  values. The notably larger  $B_{\rm EMP}$  values obtained here compared to those observed in epitaxial quantum wells are due to the confined exciton wave functions in the QDs.

The substantial effective magnetic field induced by the EMP could have a significant effect on the doped QD energy levels and carrier dynamics. Specifically, a magnetic field can mix the bright and dark states and increase the recombination rates of the dark excitons. [13] Temperature-induced thermalization can lead to redistributions of exciton populations in the bright and dark states and consequently changes in the overall decay rates. [48,49] These effects are highly dependent on the electronic fine structures of the bright triplet states as well as the energy splitting  $\Delta_{\rm DB}$  between the bright and dark states. Hence, temperature-dependent PL dynamics studies can help reveal the influence of the induced magnetic fields on the electronic fine structures. [13,48,49]

A representative PL decay curve of an undoped QD sample at 5 K is shown at the top of Figure 3a. A clear biexponential behavior can be observed with the slow component being on the time scale of around 100 ns and the fast component on sub-nanosecond scale. The fast and slow components observed in perovskite QDs are commonly assigned to radiations associated with the bright and dark states, respectively (Figure 3c, inset).[13,14] At low temperatures, thermal mixing between the bright and dark states is mostly inhibited due to minimal phonon populations at the relevant energies. The dark states, which have negligible oscillator strength, contribute to the slow components in the decay curves while the bright states dominate in the emission due to their much faster decay rates that shape the fast component. As the temperature increases, the slow component shortens considerably while the fast component almost disappears (Figure 3a), which is likely caused by increased thermalization of excitons between the bright and

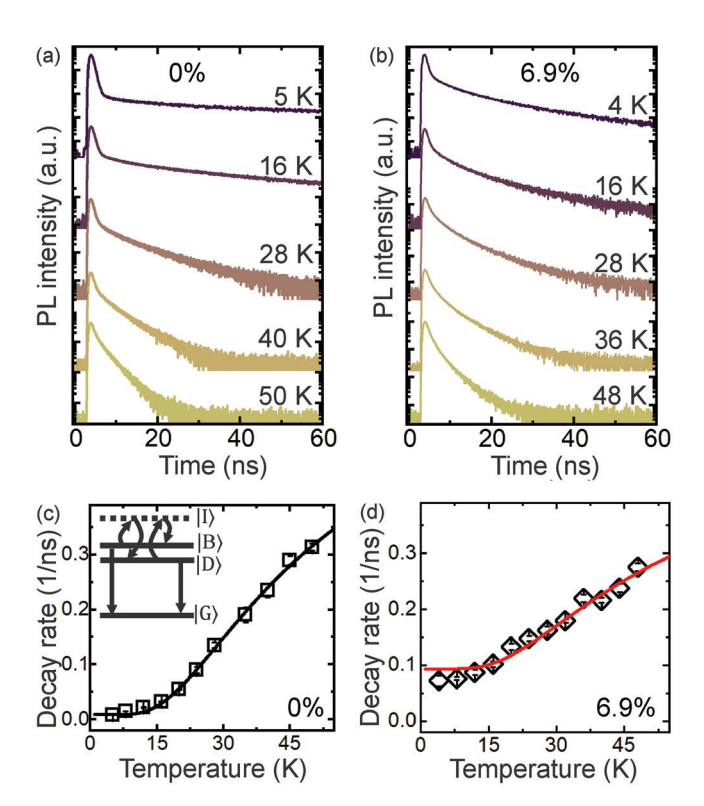


**Figure 3.** Temperature-dependent carrier dynamics. a,b) Representative decay curves of the undoped QDs (a) and QDs doped with 6.9% Mn<sup>2+</sup>ions (b). c,d) Temperature-dependent decay rates of the long components of the undoped QDs (c) and QDs doped with 6.9% Mn<sup>2+</sup>-ions (d). The curves are fittings based on the three-level model. Inset: schematic of the band-edge energy levels including the bright (|B)) and the dark (|D)) states. |G): ground state; |I): intermediate level involved in the phononassisted relaxation process between the dark and bright states.

dark states. Fitting the decay curves yields the temperaturedependent decay rates for the slow component shown in Figure 3c. Because the fast component is within the time resolution of our time-resolved PL setup, which makes the accurate derivation of the corresponding decay rates challenging, we therefore focus our discussion on the slow component. We perform similar lifetime measurements on the doped QDs. Figure 3b shows a representative group of decay curves from a QD sample doped with 6.9% Mn<sup>2+</sup>-ions. Similar to the decay curves of the undoped QDs, slow and fast components can be observed for those from the doped QDs, as well as a temperature-induced shortening in the slow components (Figure 3d), although the slow components are apparently faster than those in the undoped QDs. Since the temperature-dependent carrier dynamics of the doped QDs are not only affected by the thermalization of excitons as those in the undoped QDs, but also the existence of an intrinsic magnetic field caused by the Mn<sup>2+</sup>-ions, we infer that the difference in the carrier dynamics observed in the two types of QDs is related to the  $B_{\rm EMP}$  in the doped QDs.

To better understand the temperature-dependent carrier dynamics, we apply a model based on a three-level system<sup>[13,49]</sup> (Figure 3c, inset) in which the slow and fast components of the decay curves are closely related to the decay rates of the bright and dark states as well as the energy splitting and thermal

relaxation rates between them (Section S3, Supporting Information). Since the energy splitting in the QDs is highly associated with the magnetic fields they experience, this method allows us to determine the influence of the intrinsic magnetic fields created by the EMP. The model also takes into account the prohibited thermal relaxation between the dark and bright states at low temperatures.<sup>[13]</sup> Using this model, the temperaturedependent changes in the decay rates of the long components can be well reproduced (Figure 3c,d). Moreover, we are able to derive the intrinsic effective magnetic fields induced by the Mn<sup>2+</sup>-ions. For the QDs doped with 6.9% Mn<sup>2+</sup>-ions shown in Figure 3b,d, a  $B_{\text{FMP}}$  value of 18.6 T is obtained, which is close to the result obtained from the temperature-dependent spectral shifts in Figure 2a-d. Moreover, this  $B_{\rm EMP}$  result is consistent with the value we derived from a well-accepted "exchange box" model, [50] in which an effective hole localization volume is defined so that the Mn<sup>2+</sup>-ions within this volume interact equally strongly with the hole (see Section S4, Supporting Information for details).

We apply the same carrier dynamics method to derive the  $B_{\rm EMP}$  values of the QDs doped with various concentrations of Mn<sup>2+</sup>-ions. The results are plotting in Figure 2e (blue dots) and a good agreement between the values obtained from the two methods, namely the temperature-dependent PL spectral shifts and carrier dynamics, are observed. These two independent methods are used to separately derive the  $B_{\rm EMP}$  values and serve as a means to confirm the accuracy of the obtained  $B_{\rm EMP}$  values. The existence of EMP also explains the faster decay rates and the more prominent contributions of the slow components observed in the doped QDs in Figure 3b. The effective magnetic field induced by the EMP can cause a mixing between the bright and dark states, allowing the dark states to obtain oscillator strength at the expense of the bright state oscillator strength. [49]

Aside from confirming the existence of the intrinsic magnetic fields in the doped QDs, fitting the temperature-dependent decay rates with the three-level model further allows us to derive the electronic fine structures of the QDs. One of the most prominent parameters that determines the optical properties of the QDs is the zero-field energy splitting between the dark and bright states  $\Delta_0$ . Since the value of  $\Delta_0$  should remain mostly intact upon Mn<sup>2+</sup>-ion doping, we are able to obtain an average value of  $\overline{\Delta_0} = 5.4 \pm 0.27$  meV from the studied QDs, a value that is consistent with previous reports.<sup>[49]</sup> We are also

able to derive the bright-dark splitting  $\Delta_{\rm DB}$  under the influence of the effective magnetic fields from the fitting, the results of which are plotted as a function of  $B_{\rm EMP}$  and the doping concentration in **Figure 4**a (black). With an increase in the doping concentration and consequently the effective magnetic field  $B_{\rm EMP}$ , the dark-bright splitting increases. Another significant parameter impacts the electronic fine structures of the QDs is the Zeeman splitting. For the doped QDs, their Zeeman splitting have two major contributions:  $E_{\rm Z, total} = E_{\rm Z, int} + E_{\rm Z, EMP}$ . Here,  $E_{\rm Z, int} = g_{\rm exc} \, \mu_{\rm B} B$  is the Zeeman splitting due to the intrinsic g-factor,  $g_{\rm exc}$ , of the excitons in the QDs, of which we assume to be 2.4;  $E_{\rm Z, EMP} = 2\,CB_{\rm 5/2} \left(\frac{5\,\mu_{\rm B}\,g_{\rm Mn}\,B}{2k_{\rm B}\,T}\right)$  accounts for the Zeeman

splitting caused by the exchange field of the excitons. Figure 4a shows the Zeeman splitting  $E_{Z,int}$  related to the intrinsic g-factor of excitons (blue dots) and it increases with the effective magnetic field. A similar trend is expected for the Zeeman splitting  $E_{Z,EMP}$  caused by the exchange field.

These findings allow us to derive a more comprehensive picture of the electronic fine structures in the doped CsPbBr<sub>3</sub> QDs. At low temperatures, there are predominantly two types of crystalline structures in CsPbBr3 QDs, namely the tetragonal and orthorhombic phases.<sup>[52]</sup> Given the relatively low doping levels of the QDs used in this study, we assume that they possess similar crystalline structures as the undoped QDs. Compared to perovskite QDs with a cubic phase, those with a tetragonal phase have a lower crystal structure symmetry. In this case, although the exciton ground level of the QDs remains a dark singlet state  $|0^D\rangle$ , the originally triply degenerate bright states observed in the cubic phase are split into doubly degenerate bright states  $|1^{\pm}\rangle$  and a bright state  $|0^{B}\rangle$  (Figure 4b). A further reduction in the crystal structure symmetry leads to the orthorhombic phase, the bright states of which are split into three bright states (Figure 4c). Doping of the QDs with Mn<sup>2+</sup>ions leads to effective magnetic fields in them, which consequently increases the dark-bright splitting  $\Delta_{DB}$  and induces Zeeman splitting, as illustrated in Figure 4b,c. An increase in the Mn<sup>2+</sup>-ion doping concentration could result in larger  $B_{EMP}$ and increased dark-bright splitting  $\Delta_{DB}$  in the QDs' electronic structures. In the event that the induced effective magnetic field lies parallel to the z-crystal axis of the QD, coupling between

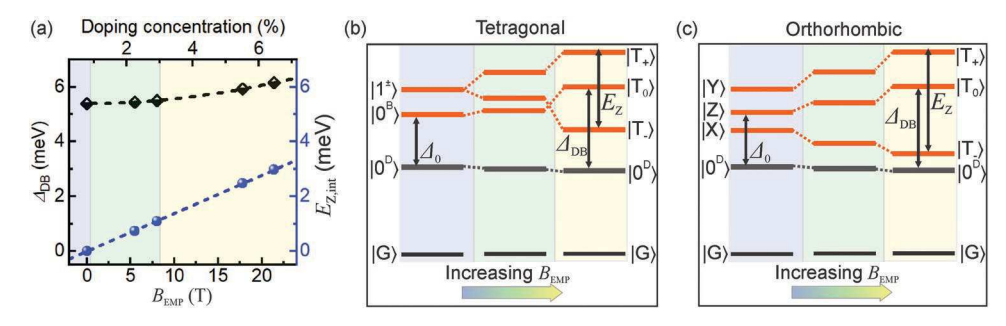


Figure 4. Effective magnetic field-induced electronic structure changes. a) Dark-bright energy splitting  $\Delta_{DB}$  (black dots) and Zeeman splitting due to the intrinsic g-factor,  $g_{exc}$ , of the excitons (blue dots) in the QDs with various doping concentrations obtained from modeling the carrier dynamics based on the three-level system. The black dashed curve is a fitting of the  $\Delta_{DB}$  data using  $\Delta_{DB} = \sqrt{\Delta_0^2 + (g_{exc} \ \mu_B \ B_{EMP})^2}$ , while the blue dashed line is a linear fit of the Zeeman splitting data. b,c) Sketches of the effective magnetic field-induced Zeeman splitting and level crossing in QDs with tetragonal and orthorhombic phases.





the dark singlet ground state  $|0^D\rangle$  and the bright state  $|0^B\rangle$  is expected, leading to the brightening of the dark state and increasing of its decay rate, as observed in Figure 3b,d. Due to the random orientations of the induced magnetic fields in the QDs with respect to their crystal axes, $^{[30]}$  we assume the coupling between the bright and dark states to be an average over various conditions. In the QDs with a tetragonal phase, a level crossing between the  $|T_0\rangle$  and  $|T_-\rangle$  bright states is expected (Figure 4b). Due to the large Zeeman splitting induced by the exchange field of the excitons, level crossing between the originally dark singlet state and the bright triplet state could also be expected. Unique to the doped QDs, they possess partially bright ground states enabled by the EMP. We expect the EMP-induced dark state brightening to be even more pronounced in smaller QDs supporting stronger EMP effects.

### 3. Conclusion

In summary, we study the temperature-dependent PL properties of CsPbBr<sub>3</sub> QDs doped with Mn<sup>2+</sup>-ions. We demonstrate that upon photon excitation, excitons in the doped QDs lead to the formation of EMP. Our analysis of the carrier dynamics reveals that the magnitude of the EMP-induced effective magnetic fields in the doped QDs increases with the Mn<sup>2+</sup>-ion doping concentrations. Consequently, the Zeeman splitting and the dark-bright splitting  $\Delta_{\mathrm{DB}}$  in the electronic fine structures of the QDs also increase with the doping level. The EMP-induced effective magnetic fields in the doped QDs can also brighten the dark singlet state, resulting in a partially bright ground state in the doped QDs. This EMP-induced ground state brightening is intrinsic to the doped QDs and does not require the existence of an external magnetic field. The findings obtained here may have two important implications. First, they would allow the creation of semiconductor nanostructures with at least partially bright ground states. Aside from the photoexcitation demonstrated in this study, EMP can also be created by electrical injection, [53] which may allow the integration of the EMP-enabled bright semiconductor nanostructures into compact optoelectronic devices. Second, the EMP-modulated singlet-triplet splitting may facilitate the development of intriguing protocols for spintronic<sup>[54]</sup> and energy harvesting<sup>[55]</sup> devices that rely heavily on the transitions between the singlet and triplet states.

# 4. Experimental Section

Temperature-Dependent Optical Measurements of the QDs: The temperature-dependent optical characterization of the QDs was performed on a home-built optical microscope. To prepare samples for the optical measurements, QD stock solutions were spin coated onto pre-cleaned quartz substrates to form uniform thin films. The thin films were then loaded into a continuous-flow liquid helium cryostat that was mounted on the microscope. A 400 nm diode laser was used to excite the samples. A microscope objective (Olympus,  $40\times$ , NA = 0.7) was used to focus the laser beam and collect emission from the samples. The collected emission was directed to a charge-coupled device mounted on a 500 mm spectrograph for imaging and spectroscopic measurements. For each sample at each temperature, PL spectra were taken from around ten different locations on the sample. Gaussian functions were used to fit the PL spectra and determine the peak positions. The

average peak positions and the associated standard errors were derived from these spectra. For time-resolved PL measurements, the pulse frequency of the diode laser was set to 0.5 or 1 MHz. Emission from the samples was focused onto single photon avalanche diodes. Time-resolved photon counting was performed with HydraHarp electronics (PicoQuant). During the temperature-dependent measurements, the samples were first cooled to 4 K and gradually warmed up. Between each temperature step, a waiting time of 10–15 min were reserved to ensure that the samples have reached thermal equilibrium.

# **Supporting Information**

Supporting Information is available from the Wiley Online Library or from the author.

# **Acknowledgements**

The authors acknowledge support from the National Science Foundation DMR Program under the award no. DMR-1905990 and DMR-1943930. Use of the Center for Nanoscale Materials, an Office of Science user facility, was supported by the U.S. Department of Energy, Office of Science, Office of Basic Energy Sciences, under Contract no. DE-AC02-06CH11357. O.C. acknowledges the support through NASA Rhode Island EPSCoR Research and Infrastructure Development Grant (NASA 80NSSC19M0045).

# **Conflict of Interest**

The authors declare no conflict of interest.

# **Data Availability Statement**

The data that support the findings of this study are available from the corresponding author upon reasonable request.

## Keywords

dark states, doping, light-induced magnetism, perovskite quantum dots, Zeeman splitting

Received: March 15, 2021 Revised: May 18, 2021 Published online:

- [1] M. V. Kovalenko, L. Protesescu, M. I. Bodnarchuk, *Science* **2017**, *358*, 745.
- [2] Y. Fu, H. Zhu, J. Chen, M. P. Hautzinger, X.-Y. Zhu, S. Jin, Nat. Rev. Mater. 2019, 4, 169.
- [3] A. Kojima, K. Teshima, Y. Shirai, T. Miyasaka, J. Am. Chem. Soc. 2009, 131, 6050.
- [4] H. Lu, J. Wang, C. Xiao, X. Pan, X. Chen, R. Brunecky, J. J. Berry, K. Zhu, M. C. Beard, Z. V. Vardeny, Sci. Adv. 2019, 5, eaay0571.
- [5] P. Odenthal, W. Talmadge, N. Gundlach, R. Wang, C. Zhang, D. Sun, Z.-G. Yu, Z. Valy Vardeny, Y. S. Li, Nat. Phys. 2017, 13, 894.
- [6] Y. Wei, Z. Cheng, J. Lin, Chem. Soc. Rev. 2018, 48, 310.
- [7] Y.-S. Park, S. Guo, N. S. Makarov, V. I. Klimov, ACS Nano 2015, 9, 10386.
- [8] H. Utzat, W. Sun, A. E. K. Kaplan, F. Krieg, M. Ginterseder, B. Spokoyny, N. D. Klein, K. E. Shulenberger, C. F. Perkinson, M. V. Kovalenko, M. G. Bawendi, *Science* 2019, 363, 1068.

- [9] C. Yin, L. Chen, N. Song, Y. Lv, F. Hu, C. Sun, W. W. Yu, C. Zhang, X. Wang, Y. Zhang, M. Xiao, *Phys. Rev. Lett.* **2017**, *119*, 026401.
- [10] G. Rainò, G. Nedelcu, L. Protesescu, M. I. Bodnarchuk, M. V. Kovalenko, R. F. Mahrt, T. Stöferle, ACS Nano 2016, 10, 2485.
- [11] M. A. Becker, R. Vaxenburg, G. Nedelcu, P. C. Sercel, A. Shabaev, M. J. Mehl, J. G. Michopoulos, S. G. Lambrakos, N. Bernstein, J. L. Lyons, T. Stöferle, R. F. Mahrt, M. V. Kovalenko, D. J. Norris, G. Rainò, A. L. Efros, *Nature* 2018, 553, 189.
- [12] P. C. Sercel, J. L. Lyons, D. Wickramaratne, R. Vaxenburg, N. Bernstein, A. L. Efros, Nano Lett. 2019, 19, 4068.
- [13] P. Tamarat, M. I. Bodnarchuk, J.-P. Trebbia, R. Erni, M. V. Kovalenko, J. Even, B. Lounis, Nat. Mater. 2019, 18, 717.
- [14] K. Xu, J. F. Vliem, A. Meijerink, J. Phys. Chem. C 2019, 123, 979.
- [15] M. Baranowski, P. Plochocka, Adv. Energy Mater. 2020, 10, 1903659.
- [16] D. Luo, R. Su, W. Zhang, Q. Gong, R. Zhu, Nat. Rev. Mater. 2020, 5, 44.
- [17] K. Lin, J. Xing, L. N. Quan, F. Pelayo García de Arquer, X. Gong, J. Lu, L. Xie, W. Zhao, D. Zhang, C. Yan, W. Li, X. Liu, Y. Lu, J. Kirman, E. H. Sargent, Q. Xiong, Z. Wei, *Nature* 2018, 562, 245.
- [18] M. T. E. Fadaly, A. Dijkstra, J. R. Suckert, D. Ziss, M. A. J. van Tilburg, C. Mao, Y. Ren, V. T. van Lange, K. Korzun, S. Kölling, M. A. Verheijen, D. Busse, C. Rödl, J. Furthmüller, F. Bechstedt, J. Stangl, J. J. Finley, S. Botti, J. E. M. Haverkort, E. P. A. M. Bakkers, *Nature* 2020, 580, 205.
- [19] M. Nirmal, D. J. Norris, M. Kuno, M. G. Bawendi, Al. L. Efros, M. Rosen, Phys. Rev. Lett. 1995, 75, 3728.
- [20] X.-X. Zhang, T. Cao, Z. Lu, Y.-C. Lin, F. Zhang, Y. Wang, Z. Li, J. C. Hone, J. A. Robinson, D. Smirnov, S. G. Louie, T. F. Heinz, Nat. Nanotechnol. 2017, 12, 883.
- [21] B. F. Habenicht, O. V. Prezhdo, Phys. Rev. Lett. 2008, 100, 197402.
- [22] S. Ghosh, S. M. Bachilo, R. A. Simonette, K. M. Beckingham, R. B. Weisman, *Science* 2010, 330, 1656.
- [23] X. Ma, N. F. Hartmann, J. K. S. Baldwin, S. K. Doorn, H. Htoon, Nat. Nanotechnol. 2015, 10, 671.
- [24] R. Beaulac, L. Schneider, P. I. Archer, G. Bacher, D. R. Gamelin, Science 2009, 325, 973.
- [25] A. A. Maksimov, G. Bacher, A. McDonald, V. D. Kulakovskii, A. Forchel, *Phys. Rev. B* **2000**, *62*, R7767.
- [26] D. R. Yakovlev, W. Ossau, in Introduction to the Physics of Diluted Magnetic Semiconductors, Springer-Verlag, Berlin 2010.
- [27] J. Seufert, G. Bacher, M. Scheibner, A. Forchel, Phys. Rev. Lett. 2002, 88, 027402.
- [28] A. K. Bhattacharjee, C. Benoit à la Guillaume, Phys. Rev. B 1997, 55, 10613
- [29] G. Mackh, W. Ossau, D. R. Yakovlev, A. Waag, G. Landwehr, R. Hellmann, E. O. Göbel, *Phys. Rev. B* **1994**, *49*, 10248.
- [30] Ł. Kłopotowski, Ł. Cywiński, P. Wojnar, V. Voliotis, K. Fronc, T. Kazimierczuk, A. Golnik, M. Ravaro, R. Grousson, G. Karczewski, T. Wojtowicz, *Phys. Rev. B* 2011, 83, 081306(R).
- [31] H. D. Nelson, L. R. Bradshaw, C. J. Barrows, V. A. Vlaskin, D. R. Gamelin, ACS Nano 2015, 9, 11177.

- [32] L. Protesescu, S. Yakunin, M. I. Bodnarchuk, F. Krieg, R. Caputo, C. H. Hendon, R. X. Yang, A. Walsh, M. V. Kovalenko, *Nano Lett.* 2015, 15, 3692.
- [33] S. Das Adhikari, A. K. Guria, N. Pradhan, J. Phys. Chem. Lett. 2019, 10, 2250.
- [34] W. Chang, D. N. Congreve, E. Hontz, M. E. Bahlke, D. P. McMahon, S. Reineke, T. C. Wu, V. Bulović, T. V. Voorhis, M. A. Baldo, *Nat. Commun.* 2015, 6, 6415.
- [35] H. Lu, X. Chen, J. E. Anthony, J. C. Johnson, M. C. Beard, J. Am. Chem. Soc. 2019, 141, 4919.
- [36] H. Uoyama, K. Goushi, K. Shizu, H. Nomura, C. Adachi, *Nature* 2012, 492, 234.
- [37] E. Elzner, L. A. Martínez-Martínez, J. Yuen-Zhou, S. Kéna-Cohen, Sci. Adv. 2019, 5, eaax4482.
- [38] M. Imran, V. Caligiuri, M. Wang, L. Goldoni, M. Prato, R. Krahne, L. De Trizio, L. Manna, J. Am. Chem. Soc. 2018, 140, 2656.
- [39] T. Cai, J. Wang, W. Li, K. Hills-Kimball, H. Yang, Y. Nagaoka, Y. Yuan, R. Zia, O. Chen, Adv. Sci. 2020, 7, 2001317.
- [40] R. A. Schneidt, C. Atwell, P. V. Kamat, ACS Mater. Lett. 2019, 1, 8.
- [41] W. Liu, Q. Lin, H. Li, K. Wu, I. Robel, J. M. Pietryga, V. I. Klimov, J. Am. Chem. Soc. 2016, 138, 14954.
- [42] J. Seufert, G. Bacher, M. Scheibner, A. Forchel, S. Lee, M. Dobrowolska, J. K. Furdyna, Phys. Rev. Lett. 2001, 88, 027402.
- [43] R. Saran, A. Heuer-Jungemann, A. G. Kanaras, R. J. Curry, Adv. Opt. Mater. 2017, 5, 1700231.
- [44] M. Cardona, Solid State Commun. 2005, 133, 3.
- [45] X. Ma, S. Cambré, W. Wenseleers, S. K. Doorn, H. Htoon, Phys. Rev. Lett. 2017, 118, 027402.
- [46] W. D. Rice, W. Liu, V. Pinchetti, D. R. Yakovlev, V. I. Klimov, S. A. Crooker, Nano Lett. 2017, 17, 3068.
- [47] Ł. Kłopotowski, Ł. Cywiński, M. Szymura, V. Voliotis, R. Grousson, P. Wojnar, K. Fronc, T. Kazimierczuk, A. Golnik, G. Karczewski, T. Wojtowicz, *Phys. Rev. B* 2013, 87, 245316.
- [48] O. Labeau, P. Tamarat, B. Lounis, Phys. Rev. Lett. 2003, 90, 257404.
- [49] L. Chen, B. Li, C. Zhang, X. Huang, X. Wang, M. Xiao, Nano Lett. 2018. 18, 2074.
- [50] P. S. Dorozhkin, A. V. Chernenko, V. D. Kulakovskii, A. S. Brichkin, A. A. Maksimov, H. Schoemig, G. Bacher, A. Forchel, S. Lee, M. Dobrowolska, J. K. Furdyna, *Phys. Rev. B* **2003**, *68*, 195313.
- [51] D. Canneson, E. V. Shornikova, D. R. Yakovlev, T. Rogge, A. A. Mitioglu, M. V. Ballottin, P. C. M. Christianen, E. Lhuillier, M. Bayer, L. Biadala, *Nano Lett.* 2017, 17, 6177.
- [52] M. Fu, P. Tamarat, H. Huang, J. Even, A. L. Rogach, B. Lounis, *Nano Lett.* 2017, 17, 2895.
- [53] F. Muckel, C. J. Barrows, A. Graf, A. Schmitz, C. S. Erickson, D. R. Gamelin, G. Bacher, Nano Lett. 2017, 17, 4768.
- [54] Y. Bae, K. Yang, P. Willke, T. Choi, A. J. Heinrich, C. P. Lutz, Sci. Adv. 2018. 4. eaau4159.
- [55] J. Zhou, Q. Liu, W. Feng, Y. Sun, F. Li, Chem. Rev. 2015, 115, 395